Cerebral Cortex October 2014;24:2721–2731
doi:10.1093/cercor/bht125
Advance Access publication May 19, 2013

Impact of Sex and Gonadal Steroids on Neonatal Brain Structure

Rebecca C. Knickmeyer[1], Jiaping Wang[4], Hongtu Zhu[2], Xiujuan Geng[5], Sandra Woolson[1], Robert M. Hamer[1,2], Thomas Konneker[6], Martin Styner[1,3] and John H. Gilmore[1]

[1]Department of Psychiatry, [2]Department of Biostatistics, [3]Department of Computer Science, University of North Carolina at Chapel Hill, Chapel Hill, NC, USA [4]Department of Mathematics, University of North Texas at Denton, Denton, TX, USA [5]School of Humanities, The University of Hong Kong, Hong Kong, Hong Kong and [6]Department of Biomolecular Engineering, University of California at Santa Cruz, CA, USA

Address correspondence to R. Knickmeyer, Department of Psychiatry, 343 Medical Wings C, Campus Box #7160, University of North Carolina, Chapel Hill, NC 27599-7160, USA. Email: rebecca_knickmeyer@med.unc.edu

There are numerous reports of sexual dimorphism in brain structure in children and adults, but data on sex differences in infancy are extremely limited. Our primary goal was to identify sex differences in neonatal brain structure. Our secondary goal was to explore whether brain structure was related to androgen exposure or sensitivity. Two hundred and ninety-three neonates (149 males) received high-resolution structural magnetic resonance imaging scans. Sensitivity to androgen was measured using the number of cytosine, adenine, guanine (CAG) triplets in the androgen receptor gene and the ratio of the second to fourth digit, provided a proxy measure of prenatal androgen exposure. There was a significant sex difference in intracranial volume of 5.87%, which was not related to CAG triplets or digit ratios. Tensor-based morphometry identified extensive areas of local sexual dimorphism. Males had larger volumes in medial temporal cortex and rolandic operculum, and females had larger volumes in dorsolateral prefrontal, motor, and visual cortices. Androgen exposure and sensitivity had minor sex-specific effects on local gray matter volume, but did not appear to be the primary determinant of sexual dimorphism at this age. Comparing our study with the existing literature suggests that sex differences in cortical structure vary in a complex and highly dynamic way across the human lifespan.

Keywords: androgen, gender, neonate, neuroimaging, sex

Introduction

Relative risk levels for many psychiatric disorders are dramatically different in males and females (Rutter et al. 2003). Many early onset neurodevelopmental disorders are male-biased, including autism spectrum disorders (Baird et al. 2000; Chakrabarti and Fombonne 2001), attention-deficit hyperactivity disorder (ADHD; Szatmari et al. 1989; Moffitt 1990), early onset persistent antisocial behavior (Moffitt and Caspi 2001), Tourette's syndrome (Wang and Kuo 2003), and early onset schizophrenia (Remschmidt et al. 1994). In contrast, many adolescent onset disorders are female-biased, including depression (Bebbington et al. 1998), anxiety (McLean et al. 2011), and eating disorders (Lucas et al. 1991). It has been hypothesized that the prevalence and expression of these disorders are related to sex differences in brain development.

There is a great deal of evidence for sexual dimorphism in the human central nervous system during both adulthood and childhood, although there is some debate as to whether this is independent of body, head, and total brain size. The best-replicated findings are greater volume of the cerebrum in males (Dekaban and Sadowsky 1978; Caviness et al. 1996; Giedd et al. 1996, 1997; Reiss et al. 1996; Nopoulos et al. 1997; Filipek 1999; De Bellis et al. 2001; Goldstein et al. 2001), relatively greater volume of the amygdala (Caviness et al. 1996; Good et al. 2001), putamen, and pallidum (Rijpkema et al. 2012) in males, and relatively greater volume of the caudate (Filipek et al. 1994; Caviness et al. 1996; Giedd et al. 1996, 1997) and hippocampus (Filipek et al. 1994; Caviness et al. 1996) in females. The largest study of children and adolescents carried out to date reports that only occipital gray matter (GM), putamen, and cerebellum all differed significantly by sex after adjusting for total brain volume; all being relatively larger in males (but note that neither the hippocampus nor the amygdala was included in this report; BDCG 2012). Voxel-based morphometry (VBM) studies also suggest that adult males and females show localized differences in cortical GM volume. Females have been reported to show increased GM volume adjacent to the depths of both central sulci and the left superior temporal sulcus, in right Heschl's gyrus and planum temporale, right inferior frontal and frontomarginal gyri, bilateral cingulate gyrus, precentral gyrus, and right inferior parietal lobule. Males have been reported to show increased GM volume in the bilateral medial temporal lobes (including hippocampus, amygdala, and entorhinal and perirhinal cortices), left inferior temporal gyrus, right middle temporal gyrus, right occipital lingual gyrus, the midbrain and both cerebellar hemispheres (Good et al. 2001; Chen et al. 2007; Lentini et al. 2012). A study of peripubertal children reported some similar findings: females had increased GM in planum temporale/parietal operculum, posterior lateral orbitofrontal cortex, and anterior cingulate, and males had larger volumes in amygdala, putamen, and ventral tegmental area (midbrain). This study also reported sexual dimorphisms that were not present in the adult: females had larger volumes in the medial prefrontal cortex, precuneus, and superior parietal lobule. Males had larger volumes in the hypothalamus, dorsolateral prefrontal cortex, and visual cortex (Lombardo, Ashwin, Auyeung, Chakrabarti, Taylor, et al. 2012).

In contrast to the above, data on sex differences in brain development during infancy are extremely limited, due to the challenges of carrying out and analyzing magnetic resonance imaging (MRI) data in this age group. An earlier study by our group demonstrated significant sex differences in intracranial volume (ICV), cortical GM, and cortical white matter (WM) in a sample of 74 neonates, but did not investigate localized effects on cortical GM due to power limitations (Gilmore et al. 2007). This is a critical gap in our knowledge as the perinatal period is an extremely dynamic stage of brain development, characterized by rapid elaboration of new synapses (Huttenlocher and Dabholkar 1997), exuberant dendritic (Petanjek et al. 2008) and axonal growth (Kasprian et al. 2008), and extensive myelination (Brody et al. 1987). These changes are reflected in

dramatic increases in GM and WM volumes as indexed by MRI (Gilmore et al. 2007, 2012; Knickmeyer et al. 2008) and presumably underpin the rapid maturation of motor skills, cognition, social abilities, and language that characterize the first 2 years of life (Kagan and Herschkowitz 2005). This is a critical period for childhood-onset illnesses, such as autism (Hazlett et al. 2005, 2011; Wolff et al. 2012). There is also extensive evidence that adult-onset diseases, such as schizophrenia, originate in early brain development (Rapoport et al. 2005; Fatemi and Folsom 2009). Early aberrations in neurodevelopment, relevant to adult-onset disorders, can be captured via MRI as evidenced by a recent study, showing that male neonates at high genetic risk for schizophrenia have larger intracranial, cerebrospinal fluid (CSF), total GM, and lateral ventricle volumes than controls (Gilmore et al. 2010).

Assuming that sexual dimorphism is present in the neonate brain, the question arises as to what biological mechanisms produce these differences. For many years, sexual differentiation of the brain was considered to be analogous to that of the reproductive tracts, such that in the presence of testicular hormones (in particular testosterone) discrete male neural circuits would develop in an otherwise sexually monomorphic brain, while in the absence of testosterone discrete female neural circuits would develop. However, recent evidence suggests that a more complex and nuanced model is necessary (McCarthy and Arnold 2011). First, in contrast to the reproductive tracts, sexual dimorphism in the brain is generally a difference of degree with a substantial overlap in the distributions of males and females (Breedlove 1994; McCarthy and Arnold 2011). This suggests that, instead of distinct male and female neural circuits, there are shared networks that are differentially weighted toward sex-typical responses (McCarthy and Arnold 2011). Thus, the relative amount of testosterone (rather than the presence or absence of testosterone) exposure may produce an average difference between the sexes and contribute to individual differences within each sex. This model is supported by a recent study, which reported that individual differences in fetal testosterone levels measured in amniotic fluid are associated with sexually dimorphic GM volumes in peripubertal males, including the right temporoparietal junction/posterior temporal sulcus, planum temporale/parietal operculum, and posterior lateral orbitofrontal cortex (Lombardo, Ashwin, Auyeung, Chakrabarti, Taylor, et al. 2012). Secondly, there is a growing recognition that nonhormonal mechanisms such as direct sex-chromosome effects and sex-specific environments play an important role in sexual differentiation of the brain.

The primary goal of the current study was to identify sex differences in brain development in neonates using automated region of interest (ROI) volumetry and tensor-based morphometry (TBM). We chose to use TBM rather than classic VBM as false-positive findings due to systematic group differences in registration errors are less likely (Hua et al. 2008; Lepore et al. 2008). TBM analyses were restricted to GM. Localized WM changes are also of interest, but we felt that these would be best addressed through diffusion tensor imaging. The secondary goal of the current study was to explore whether individual differences in brain volumes within sexually dimorphic areas were related to androgen exposure or sensitivity. A genetic predisposition for high sensitivity to T was measured using the number of cytosine, adenine, guanine (CAG) triplets in the androgen receptor gene, low numbers of CAG triplets are associated with greater receptor sensitivity/efficiency (Chang 2002), and the ratio of the second to fourth digit (2D:4D) was taken as a proxy measure of prenatal testosterone exposure (FT) (Manning et al. 1998). We note that a longitudinal study of 2D:4D ratios at birth, 1 year, and 2 years of age carried out by our group showed a lack of stability across age. Therefore, in this analysis, we only included digit ratios collected in a narrow age band (around 2 weeks of age), an age point which showed significant sex differences in our previous work (Knickmeyer et al. 2011). We also note that our analysis is based on the previously discussed model in which sexual dimorphism arises from differences in the relative amount of testosterone. A study of typically developing children such as this cannot rule out the possibility that sexual differentiation of the neonate brain is determined by the presence or absence of testosterone in a completely binary fashion.

Materials and Methods

Subjects

Two hundred and ninety-three neonates including 149 males and 144 females, and 143 singletons and 150 twins. Mothers were recruited during the second trimester of pregnancy from the outpatient obstetrics and gynecology clinics at UNC hospitals. Exclusion criteria at enrollment were the presence of abnormalities on fetal ultrasound or major medical illness in the mother. Demographic data are found in Table 1. Note that with the exception of maternal ethnicity (METHNIC), males and females did not differ significantly on any of the demographic variables examined. This study was approved by the Institutional Review Board of the University of North Carolina (UNC) School of Medicine. Written informed consent was obtained from the participants' mothers before study procedures were carried out.

Image Acquisition

MRI was carried out at the UNC MRI Research Center on a Siemens head-only 3-T scanner (Allegra, Siemens Medical

Table 1
Demographic data

Variable	Male	Female
Gestational age at birth (days) mean (SD), range	264.9 (14.78), 224–292	264.7 (15.86), 224–295
Birthweight (g) mean (SD), range	2973 (664.1), 1553–4650	2895 (537.9), 1781–4295
Gestational age at MRI (days) mean (SD), range	292.5 (12.92), 261–324	295.4 (20.09), 263–401
Maternal age at birth (years) mean (SD), range	30.24 (5.68), 17–48	30.47 (5.58), 18–44
Paternal age at birth (years) mean (SD), range	31.24 (5.48), 20–41	31.94 (6.14), 19–47
Maternal education level (years) mean (SD), range	15.32 (3.13), 8–24	15.46 (2.96), 8–24
Total household income (dollars) mean (SD), range	$68 029 ($46 452), 0–$237 000	$72 147 ($52 347), 0–$280 000
Twin status		
Singleton no. (%)	72 (48.32)	71 (49.31)
Twin no. (%)	77 (51.68)	73 (50.69)
Maternal ethnicity*		
White no. (%)	119 (79.87)	107 (74.31)
Black or African American no. (%)	21 (14.09)	35 (24.31)
Asian no. (%)	8 (5.37)	2 (1.39)
American Indian or Alaskan Native no. (%)	1 (0.67)	0 (0)

*$P = 0.02$ (different between males and females).

System, Inc., Erlangen, Germany) as previously described (Gilmore et al. 2007). All subjects were studied without sedation. Once a child was asleep, he/she was fitted with earplugs and placed in the MRI scanner with a head in a Vac-Fix immobilization device, and additional foam padding to diminish the sounds of the scanner. Scans were carried out with a neonatal nurse present, and a pulse oximeter was used to monitor heart rate and oxygen saturation. T_1-weighted images were obtained using a 3-dimensional (3D) spoiled gradient (FLASH repetition time [TR]/echo time [TE]/flip angle 15/7 ms/25°). Proton density and T_2-weighted images were obtained with a turbo spin echo sequence (TSE TR/TE1/TE2/flip angle 6200/20/119 ms/150°). Spatial resolution was $1 \times 1 \times 1$ mm^3 voxel size for T_1-weighted images and $1.25 \times 1.25 \times 1.5$ mm^3 voxel size with a 0.5-mm interslice gap for proton density/T_2-weighted images.

Automated Region of Interest Volumetry

Brain tissue was classified as GM, unmyelinated WM, myelinated WM (mWM), and CSF using an automatic, atlas-moderated expectation maximization segmentation tool as previously described (Prastawa et al. 2005; Gilmore et al. 2007). Parcellation of each subject's brain into regions was achieved by nonlinear warping of a parcellation atlas template as previously described (Hazlett et al. 2005; Gilmore et al. 2007; Knickmeyer et al. 2008). Left and right hemispheres were subdivided into 4 regions along the anterior–posterior axis (roughly corresponding to prefrontal, frontal, parietal, and occipital regions). Note that portions of the temporal lobe are included in each section (primarily frontal and parietal). The cerebellum, brainstem, and subcortical structures are represented separately. Note that subcortical structures are combined into a single "exclusion" area; individual subcortical structures cannot be reliably defined at this age. After deformation, the parcellation template is combined with the tissue classification maps and results in estimates of GM, WM, mWM, and CSF for each region. The volume of mWM in the cortex was very small and likely represented partial-volume effects; therefore, we did not perform statistical tests on cortical mWM. The neonatal lateral ventricles are segmented using ITK-SNAP (Insight Toolkit SNAP) a semi-automated 3D segmentation tool, which uses a level-set evolution method (Yushkevich et al. 2006). SNAP is controlled by both a user-defined initialization and by data-specific segmentation protocols with region-growing parameters that operate in conjunction with the probabilistic CSF map generated during tissue segmentation. Analysis was restricted to the following variables: ICV, total GM, total WM, total CSF, lateral ventricle volume, cerebellar volume, and lobar GM and WM (14 volumes total).

Tensor-Based Morphometry: Image Preprocessing

Brain tissue was extracted from the original T_2-weighted images and corrected for intensity inhomogeneity using an expectation maximization segmentation algorithm (Prastawa et al. 2005). T_2-weighted images were used as these had better signal-to-noise ratio in our neonatal sample. The skull stripped images were then rigidly aligned to match the center and orientation, and the average image was calculated afterwards, serving as the template of the following affine alignment. The rigid and affine registrations were employed with the AFNI software (Cox 1996). Intensity histogram matching was then applied on the affine aligned images to prepare for the nonrigid registration. The unbiased large deformation nonrigid group-wise registration method (Joshi et al. 2004) was used to construct the atlas and estimate deformation fields mapping each input images to the atlas. To get the final transformation from the original image space to the atlas space, we composed the affine transformation matrix and the nonrigid deformation field.

CAG Repeats

DNA was extracted from buccal samples using standard methods as described in the Puregene® DNA Purification Kit (Gentra Systems) using supplies from Qiagen. After extraction, samples were aliquoted into 2 (23 µL) tubes and stored at −80° C. Prior to freezing, DNA quantity and quality (indexed by the 260/280 nm ratio) were assessed by spectrophotometer (Beckman DU640, Beckman-Coulter, Brea, CA, USA). To genotype the CAG repeat polymorphism in the human androgen receptor gene, we adapted a protocol from Allen et al. (1992). First, a polymerase chain reaction (PCR) spanning the CAG repeat polymorphism was performed. The forward primer was 1, 5′-FAM-GCTGTGAAGGTTGCTGTTCCTCAT-3′, and the reverse primer was 2, 5′-TCCAGAATCTGTTCCAGAGCGTGC-3′. The PCR was carried out on a MJ Research PTC-2000 Thermocycler. The PCR product was purified using a Promega Wizard SV 96 PCR clean-up system using the standard protocol. The size of the PCR fragments for each sample were measured using a 3730 DNA Analyzer (Applied Biosystems, Foster City, CA) using the 600LIZ size standard for comparison. Only PCR products with a carboxyfluorescein-labeled end are detected by the analyzer. The data were viewed using the GeneMapper software (Applied Biosystems) to determine the peak fragment length for each sample. Genotypes were called by visual observation of the peak fragment length within the GeneMapper software. Peak fragment lengths were then converted to the CAG repeat number. The overall no-call percentage for genotypes was 2%. Ninety-eight samples were run in duplicate to check for genotyping disagreements. Two samples did not replicate (a rate of 2%), probably due to a pipetting error. Additional genotyping was performed to resolve the genotype in these individuals. In total, CAG repeat length was available for 262 children. For females, who have 2 copies of the androgen receptor gene, mean CAG length was used in subsequent statistical analyses.

2D:4D Ratio

We collected black and white photocopies of both the left and right hands of participating children at the neonatal MRI visit. Measurements of second and fourth digit length were taken from photocopies using vernier calipers with an accuracy of ±0.02 mm and repeatability of 0.01 mm. The 2D:4D ratio was calculated from digit length measured from the basal crease of the digit proximal to the palm to the tip of the digit. Each digit was measured twice with a minimum of 1 day between measurements. A single rater performed all 2D:4D measurements. Intraclass correlation coefficients (Shrout-Fleiss fixed set) for this rater are 0.86 and 0.90 (for left and right hands, respectively). For all subsequent analyses, 2D:4D ratios were calculated using the average of the 2 measurements. The rater was blind to subject's sex. While the rater was not given explicit information as regards subject age or ethnicity, the photocopies themselves provide some limited information relevant to these parameters (e.g. size and shape of the hand, skin tone). Right versus left hand could be determined from the

Table 2
Descriptive data for testosterone exposure variables

Variable	Male	Female	*P*-value
2D:4D ratio right mean (SD), range	0.92 (0.04), 0.84–1.02	0.93 (0.05), 0.82–1.03	0.08
2D:4D ratio left mean (SD), range	0.92 (0.04), 0.80–1.01	0.93 (0.04), 0.85–1.03	0.04
CAG repeats mean (SD), range	19.77 (2.71), 12.00–28.00	19.58 (2.29), 14.50–25.50	0.60

photocopies themselves. The sequence of images was randomized. Left 2D:4D was available for 210 subjects, and right 2D:4D was available for 209 subjects (see Table 2 for descriptive statistics on CAG repeat and digit ratios).

Data Analysis

For demographic and descriptive data as well as the results of automated ROI volumetry, statistical analyses were performed using the SAS statistical software, version 9.2. Mixed models were used to study the relationship between brain volumes, sex, CAG repeat length, and digit ratios. Mixed models methodology was used to treat twins as repeated measures, whereas singletons had no repeated measures. In other words, twin pairs were treated as a single subject. The compound symmetry covariance structure was used to capture the correlation between twins in a pair (with only 2 twins in a pair there is only 1 off-diagonal correlation; Munoz et al. 1986). All models were adjusted for gestational age at MRI and METHNIC. We used METHNIC as we expected it to be more reliable than paternal ethnicity. When testing for sex differences, we ran analyses both with and without adjusting for ICV. Models testing the effect of CAG repeat and digit ratios were run separately in males and females. All statistical hypothesis tests were 2-tailed. Tests were conducted at a significance level of 0.05. We also ran 2 sensitivity analyses: one with birthweight as a covariate and another including only 1 individual from each MZ pair.

For TBM, the associations between local GM volumes, sex, CAG repeat length, and digit ratios were examined by fitting a multiscale adaptive generalized estimation equation (MAGEE) model to the Jacobian determinant of the deformation matrix at each voxel of the template (note that WM was masked and only GM was examined). The MAGEE method extends the multiscale adaptive regression model (MARM) method (Zhu et al. 2009; Li et al. 2011, 2013) to the correlated sample setting. MAGEE methodology treated the twins as repeated measures, whereas the singletons had no repeated measures. It integrates a commonly used approach for analyzing the correlated data called generalized estimation equation (GEE) with adaptive smoothing methods. GEE models account for within-twin correlation among repeated measures via the specification of a "working" correlation structure in parameter estimation. Specifically, the compound symmetry covariance structure was used to capture the correlation between twins in a pair. An attractive feature of GEE models is that the estimated regression coefficients and their associated standard deviations are valid even if the correlation structure assumed for modeling the within-twin correlation are not precisely correct (Liang and Zeger 1986).

This was a 2-step analysis. In the first step, our primary scientific interest was to localize regions which show a significant difference between males and females. In the second step, the primary interest was to localize regions which were related to CAG repeat length and the digit ratio within sexually dimorphic regions in a congruent direction (male > female sexual dimorphism and FT-positive correlation; female > male sexual dimorphism and FT-negative correlation). These models were run separately in males and females.

The final form in the first step of estimating equations in MAGEE included gender while adjusting for METHNIC, ICV, and gestational age at MRI. The final form in the second step for all male or female subjects included the variable indexing testosterone exposure (left 2D:4D, right 2D:4D, or CAG repeat) while adjusting for METHNIC, ICV, and gestational age at MRI. To clarify the details, we interpret these comparisons in statistics context. For the comparison of males versus females, we will set up a linear model:

$$\begin{aligned} y(d) = {} & \beta 0 \cdot 1 + \beta 1 \cdot \text{gender} + \beta 2 \cdot \text{age} + \beta 3 \cdot 1(\text{METHNIC} \\ & = \text{White}) + \beta 4 \cdot 1(\text{METHNIC} \\ & = \text{Asian}) + \beta 5 \cdot 1(\text{METHNIC} = \text{Black}) + \beta 6 \cdot \text{ICV} \end{aligned}$$

$y(d)$ is the imaging measure at the dth voxel and $\mathbf{1}(\cdot)$ is an indicator function for METHNIC. We are interested in the estimation of the coefficient $\beta 1$ and testing whether $\beta 1 = 0$ is statistically significant or not. The value of $\beta 1$ can be negative or positive across the whole brain. At a specific voxel, if it is positive, it indicates that the imaging measure in females is statistically higher than that in males, denoted as female > male; otherwise, female is statistically lower than male, denoted as female < male. Models for the second step are similar. For example, to examine the influence of CAG repeat, we will set up the linear model:

$$\begin{aligned} y(d) = {} & \beta 0 \cdot 1 + \beta 1 \cdot \text{CAG repeat} + \beta 2 \cdot \text{age} + \beta 3 \cdot 1(\text{METHNIC} \\ & = \text{White}) + \beta 4 \cdot 1(\text{METHNIC} \\ & = \text{Asian}) + \beta 5 \cdot 1(\text{METHNIC} = \text{Black}) + \beta 6 \cdot \text{ICV} \end{aligned}$$

Analyses for the second step were restricted to relevant regions identified in the first step (Fig. 1). In total, the secondary analyses included the following comparisons:

1. Regions where males > females and negative correlation with CAG repeat in males.
2. Regions where males > females and negative correlation with CAG repeat in females.
3. Regions where males > females and negative correlation with left 2D:4D in males.
4. Regions where males > females and negative correlation with left 2D:4D in females
5. Regions where males > females and negative correlation with right 2D:4D in males.
6. Regions where males > females and negative correlation with right 2D:4D in females
7. Regions where females > males and positive correlation with CAG repeat in males.
8. Regions where females > males and positive correlation with CAG repeat in females.
9. Regions where females > males and positive correlation with left 2D:4D repeat in males.
10. Regions where females > males and positive correlation with left 2D:4D repeat in females.

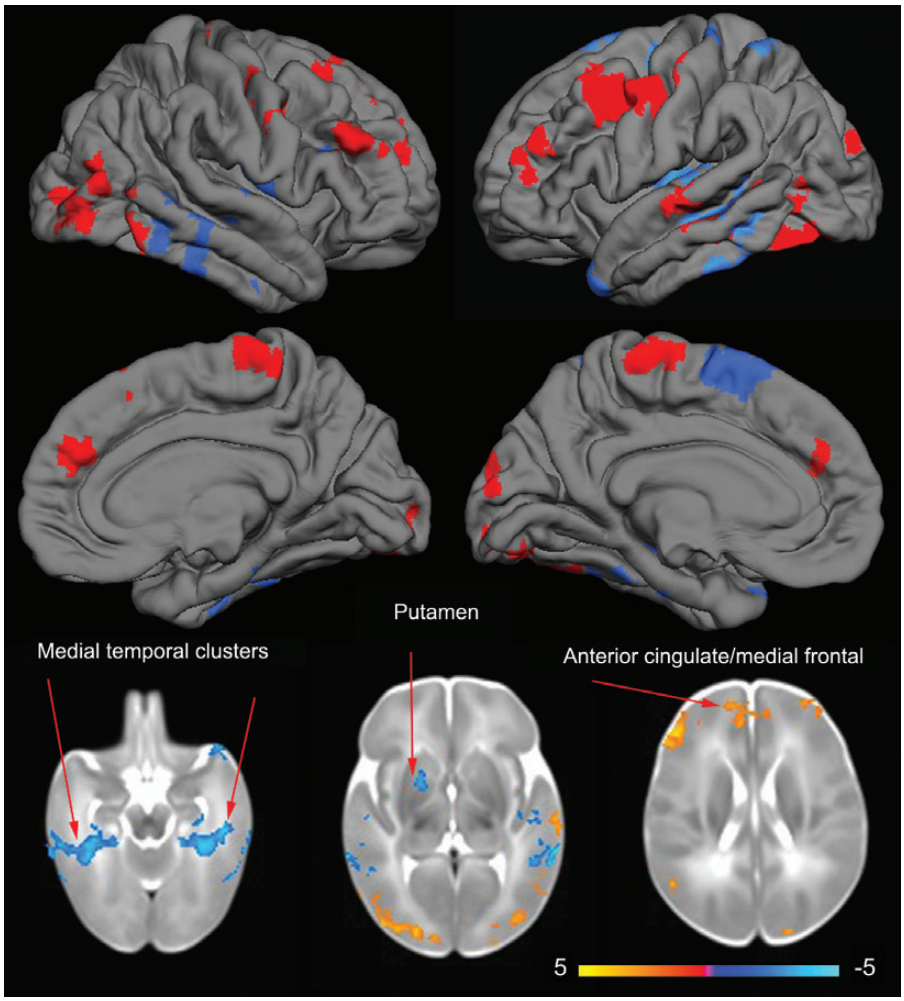

Figure 1. Sex effects on local GM volume (TBM). Upper images show significant sex differences in local GM volumes projected onto surface-rendered views of the left and right hemispheres, lateral view (top), and medial view (middle). Clusters where females > males are in red, and clusters where males > females are in blue. Bottom images are selected 2-dimensional axial slices with significant clusters displayed on the atlas of the neonate brain. Color bar gives the *t*-value at each voxel. Red/yellow indicates females > males. Blue/green indicates males > females.

11. Regions where females > males and positive correlation with right 2D:4D repeat in males.
12. Regions where females > males and positive correlation with right 2D:4D repeat in females.

For all hypothesis tests, cluster-based thresholding was used to identify extended areas of signal (Cao 1999; Worsley et al. 1999; Hayasaka et al. 2004). First, we detected clusters of contiguous suprathreshold voxels at a significance level of 0.025 with cluster size threshold at $K = 100$. We then calculated a *P*-value for each cluster on the basis of its size/mass to test whether a ROI size is significant or not at the level of 0.001. Cluster-based inference is based on random field theory, a widely used multiple testing method for determining corrected significances while accounting for the high level of spatial dependencies between adjacent voxels (Worsley et al. 1996). The manual and the code of the nonstationarity correction toolbox for cluster size *P*-values are freely available at http://www.fmri.wfubmc.edu/. We also ran 2 sensitivity analyses, one with birthweight as a covariate and another including only 1 individual from each MZ pair.

Results

Sex Differences

Automated Region of Interest Volumetry

With the exception of the lateral ventricles, all absolute brain volumes were significantly greater in males than in females (Table 3). The same pattern of results was seen when including only 1 individual from each MZ twin pair and when including birthweight as a covariate, with the exception that the cerebellum was not significantly larger in males when adjusting for birthweight. There were no significant sex differences in brain volumes when adjusting for ICV (Table 4). This pattern held when including only 1 individual from each MZ twin pair and when including birthweight as a covariate.

Tensor-Based Morphometry

Adjusting for ICV, males had increased GM volumes in the bilateral medial temporal cortex (including fusiform gyrus, parahippocampus, and hippocampus), superior, middle, and inferior temporal gyri (primarily anterior), rolandic operculum,

Table 3
Sex differences in absolute brain volume (ROI volumetry)

Dependent variable	Male LS mean (SE)	Female LS mean (SE)	Percent difference (%)	*P*-value
Intracranial volume	493637 (5568)	466274 (5787)	5.87	<0.0001
Total GM	250831 (2727)	238119 (2836)	5.32	<0.0001
Total WM	170507 (2070)	161085 (2155)	5.85	<0.0001
Total CSF	61777 (1431)	56998 (1496)	8.38	0.0004
Cerebellar volume	25037 (407)	24288 (425)	3.08	0.0467
Prefrontal GM	29365 (592)	27621 (618)	6.31	0.0016
Prefrontal WM	26516 (466)	24725 (486)	7.24	<0.0001
Frontal GM	44900 (596)	42647 (623)	5.29	<0.0001
Frontal WM	40387 (559)	38409 (585)	5.51	0.0002
Parietal GM	61894 (839)	58985 (876)	4.93	0.0002
Parietal WM	50401 (728)	48044 (761)	4.91	0.0005
Occipital GM	72350 (980)	68701 (1021)	5.31	<0.0001
Occipital WM	44301 (642)	41513 (670)	6.72	<0.0001
Ventricle volume	4442 (289)	3926 (337)	13.14	0.1069

Note: Brain volumes are in mm^3, for all variables males had larger absolute volumes than females.

Table 4
Sex differences in brain volumes adjusted for ICV (ROI volumetry)

Dependent variable	Male LS mean (SE)	Female LS mean (SE)	Percent difference (%)	*P*-value
Total GM	242685 (929)	242506 (959.30)	0.07	0.84
Total WM	164583 (889)	164390 (914.80)	0.12	0.82
Total CSF	58909 (1050)	58806 (1087.41)	0.18	0.92
Cerebellar volume	24521 (374)	24583 (388.15)	0.25 (F > M)	0.86
Prefrontal GM	28357 (513)	28150 (528.43)	0.74	0.68
Prefrontal WM	25727 (393)	25192 (405.70)	2.12	0.15
Frontal GM	43632 (418)	43373 (434.16)	0.60	0.52
Frontal WM	38929 (324)	39214 (334.09)	0.73 (F > M)	0.37
Parietal GM	59822 (502)	60124 (518.32)	0.50 (F > M)	0.53
Parietal WM	48680 (463)	49028 (479.75)	0.71 (F > M)	0.44
Occipital GM	70041 (691)	69884 (712.85)	0.22	0.81
Occipital WM	42767 (462)	42278 (477.94)	1.16	0.28
Ventricle Volume	4277 (284)	4088 (330.04)	4.62	0.56

Heschl's gyrus, and insular cortex, as well as the left supplementary motor area, left medial frontal gyrus (superior), left superior frontal gyrus, left precentral and postcentral gyri, left temporal pole, right putamen and pallidum, and right frontal inferior trigonal. Females had increased GM volumes in bilateral superior and middle frontal gyri, precentral gyri, occipital cortex, inferior and middle temporal gyri (posterior), paracentral lobules, supplementary motor area (posterior), anterior cingulum, and medial frontal gyri (superior), as well as the right frontal inferior trigonal, and left superior temporal gyrus (posterior; see Table 5 for details). The pattern of results was highly similar when including birthweight as a covariate and when including only 1 individual from each MZ pair. We do note that the female > male medial frontal cluster, including anterior cingulate, did not meet our significance criterion of $P < 0.001$ in these sensitivity analyses ($P = 0.0025$ and 0.0046, respectively). In addition, the male > female clusters that included right putamen and supplementary motor cortex did not meet our significance criterion when including only 1 individual from each MZ pair ($P = 0.0015$ and 0.0020, respectively), probably due to the lower power of this analysis (Supplementary Table 1).

Gonadal Steroid Effects

Automated Region of Interest Volumetry

Because there were no significant sex differences when correcting for overall ICV, we only tested whether ICV was associated with CAG repeat number or digit ratios. CAG repeat number, right 2D:4D, and left 2D:4D did not predict ICV in either males or females in the primary analyses or in the sensitivity analyses.

Table 5
Sex differences in local GM volumes (TBM)

	Cluster size	Maximum *t*-value	Maximum *P*-value	Cluster *P*-value	Anatomical regions
Male > female	2995	5.71	<0.0001	<0.0001	Fusiform_L (1119) Temporal_Mid_L (948) Temporal_Inf_L (712) Parahippocampal_L (108) Temporal_Sup_L (94) Occipital_Inf_L (12) Insula_L (1) Supramarginal_L (1)
	2562	4.41	<0.0001	<0.0001	Fusiform_R (918) Temporal_Inf_R (829) Temporal_Mid_R (669) Parahippocampal_R (101) Temporal_Sup_R (44) Hippocampus_R (1)
	812	4.11	<0.0001	0.0001	Rolandic_Oper_R (398) Temporal_Sup_R (198) Insula_R (188) Heschl_R (28)
	808	4.22	<0.0001	<0.0001	Supp_Motor_Area_L (520) Frontal_Sup_Medial_L (124) Frontal_Sup_L (114) Frontal_Mid_L (29) Supp_Motor_Area_R (21)
	644	3.44	0.0003	0.0007	Rolandic_Oper_L (298) Heschl_L (170) Insula_L (92) Temporal_Sup_L (84)
	336	3.62	0.0002	0.0004	Postcentral_L (135) Precentral_L (128) Parietal_Sup_R (72) Frontal_Sup_L (1)
	248	3.84	0.0001	0.0002	Temporal_Pole_Sup_L (158) Temporal_Pole_Mid_L (90)
	221	3.76	0.0001	0.0002	Putamen_R (133) Pallidum_R (88)
	125	3.55	0.0002	0.0004	Frontal_Inf_Tri_R (113) Insula_R (8) Frontal_Infer_Oper_R (4)
	125	4.13	<0.0001	0.0001	Temporal_Mid_R (93) Temporal_Inf_R (26) Temporal_Sup_R (6)
	101	3.71	0.0001	0.0003	Temporal_Mid_L (55) Temporal_Inf_L (46)
Female > male	2407	5.03	<0.0001	<0.0001	Frontal_Mid_L (1451) Precentral_L (796) Frontal_Sup_L (100) Postcentral_L (26) Frontal_Inf_Tri_L (18) Frontal_Inf_Oper_L (16)
	1285	3.99	<0.0001	0.0001	Occipital_Mid_L (567) Temporal_Mid_L (293) Calcarine_L (181) Occipital_Sup_L (131) Occipital_Inf_L (77) Temporal_Inf_L (26) Lingual_L (6) Fusiform_L (3) Angular_L (1)
	1081	3.69	0.0001	0.0003	Occipital_Mid_R (563) Temporal_Mid_R (217) Occipital_Sup_R (122) Calcarine_R (122) Cuneus_R (57)
	873	3.45	0.0003	0.0006	Frontal_Mid_R (344) Precentral_R (304) Frontal_Sup_R (142) Frontal_Inf_Oper_R (74) Frontal_Sup_Medial_R (9)
	790	4.56	<0.0001	<0.0001	Frontal_Inf_Tri_R (600) Frontal_Mid_R (190)
	633	4.47	<0.0001	<0.0001	Temporal_Mid_R (413) Temporal_Inf_R (220)
	596	4.35	<0.0001	<0.0001	Supp_Motor_Area_R (319) Supp_Motor_Area_L (146) Paracentral_Lobule_L (106) Paracentral_Lobule_R (25)
	401	3.34	0.0005	0.0009	Cingulum_Ant_R (149) Frontal_Sup_Medial_R (99) Frontal_Sup_Medial_L (92) Frontal_Sup_R (35) Cingulum_Ant_L (22) Frontal_Mid_R (3) Frontal_Sup_L (1)
	335	3.82	0.0001	0.0002	Frontal_Mid_R (177) Frontal_Sup_R (151) Frontal_Sup_Medial_R (7)
	308	3.47	0.0003	0.0006	Frontal_Mid_L (260) Frontal_Inf_Tri_L (48)
	253	3.65	0.0002	0.0003	Temporal_Sup_L (151) Temporal_Mid_L (102)
	225	3.51	0.0003	0.0005	Temporal_Mid_R (156) Angular_R (60) Temporal_Sup_R (9)
	109	3.84	0.0001	0.0002	Cuneus_L (57) Occipital_Sup_L (52)

Tensor-Based Morphometry (Within Areas That are Larger in Males)

Within males, lower CAG repeat number was associated with increased volumes in the left supplementary motor area. However, this relationship was not seen in the sensitivity analyses. Within females, lower CAG repeat number was associated with increased volumes in the right inferior temporal gyrus. This relationship was also seen in the sensitivity analyses, suggesting that testosterone, acting through the androgen receptor, increases volumes of the right inferior temporal gyrus in females. In the main analyses, no negative associations were identified between left or right 2D:4D and brain volumes within cortical regions, which are greater in males than in females in either sex. Associations with the left fusiform and right inferior trigonal were seen with left 2D:4D in females in the analysis including only 1 individual from each MZ pair (Table 6 and Supplementary Tables 3 and 5).

Tensor-Based Morphometry (Within Areas That are Larger in Females)

Within males, lower CAG repeat number was associated with decreased volumes in bilateral supplementary motor areas and paracentral lobules. This relationship was seen in the sensitivity analysis adjusting for birthweight, but not in the analysis including only 1 individual from each MZ pair. Lower right 2D:4D was also associated with decreased volumes in supplementary motor areas in both the primary and sensitivity analyses. An association between left 2D:4D and supplementary motor area volume was seen in the sensitivity analysis adjusting for birthweight. Taken together, these findings suggest that testosterone, acting through the androgen receptor, decreases volumes of the bilateral supplementary motor areas and paracentral lobules in males. In females, lower CAG repeat number was associated with decreased volumes in areas of the left middle occipital gyrus and left middle temporal gyrus in both the primary and sensitivity analyses, suggesting that testosterone, acting through the androgen receptor, decreases volumes of the left middle occipital gyrus and left middle temporal gyrus in females. Additional clusters were observed in the sensitivity analyses, particularly in that which included only 1 individual from each MZ pair. These results should be treated with caution as this analysis is expected to be less powerful and stable than the primary analysis (Table 7 and Supplementary Tables 4 and 6).

Discussion

This is the first study to provide detailed information on sex differences in global, regional, and local brain volumes in the neonate. Comparing our study with similar studies in older children and adults suggests that sex differences in cortical structure vary in a complex and highly dynamic way across the human lifespan.

Taking the existing literature into account, results can be grouped into 4 general patterns: (1) Sex differences which are stable across the lifespan, (2) sex differences which are not present in the neonate but arise during childhood and/or adolescence, (3) sex differences which are present during periods of high circulating gonadal steroids (e.g. neonate and adult, but not childhood), and (4) sex differences which are unique to the neonate.

Regarding pattern 1, relatively few sexual dimorphisms appear to be stable from the perinatal period into adulthood. Automated lobar morphometry analyses revealed a robust sex difference in ICV of 5.87% (males larger than females), which accounted for all regional sexual dimorphism. This difference

Table 6
Positive associations between testosterone exposure and local GM volumes within regions where males are greater than females

	Cluster size	Maximum *t*-value	Maximum *P*-value	Cluster *P*-value	Anatomical regions
Males					
CAG	104	3.82	0.0001	0.0002	Supp_Motor_Area_L (102) Frontal_Sup_Medial_L (2)
Left 2D:4D	None				
Right 2D:4D	None				
Females					
CAG	139	4.80	<0.0001	<0.0001	Temporal_Inf_R (113) Fusiform_R (19) Temporal_Mid_R (7)
Left 2D:4D	None				
Right 2D:4D	None				

Note: Lower numbers of CAG repeats are associated with greater sensitivity to testosterone (e.g. greater exposure). Lower 2D:4D ratios are associated with higher circulating levels of testosterone (e.g. greater exposure). This means that a negative correlation with the CAG or digit ratio represents a positive association between testosterone exposure and brain volume.

Table 7
Negative associations between testosterone exposure and local GM volumes within regions where females are greater than males

	Cluster size	Maximum *t*-value	Maximum *P*-value	Cluster *P*-value	Anatomical regions
Males					
CAG	302	4.06	<0.0001	0.0001	Supp_Motor_Area_R (135) Supp_Motor_Area_L (112) Paracentral_Lobule_L (45) Paracentral_Lobule_R (10)
Left 2D:4D	None				
Right 2D:4D	164	4.51	<0.0001	<0.0001	Supp_Motor_Area_R (144) Supp_Motor_Area_L (15) Paracentral_Lobule_L (5)
Females					
CAG	188	4.40	<0.0001	<0.0001	Temporal_Mid_L (99) Occipital_Mid_L (63) Occipital_Inf_L (23) Temporal_Inf_L (3)
Left 2D:4D	None				
Right 2D:4D	None				

Note: Higher numbers of CAG repeats are associated with less sensitivity to testosterone (e.g. lower exposure). Higher 2D:4D ratios are associated with lower circulating levels of testosterone (e.g. lower exposure). This means that a positive correlation with the CAG or digit ratio represents a negative association between testosterone exposure and brain volume.

is somewhat smaller than that reported in a previous study carried out in a subset of this group (7.8%, $N = 74$). Given the much larger sample size in the current study, 5.87% is expected to be a better estimate of sex differences in the general population. We also considered the possibility that differences between the 2 studies reflected the inclusion of twin births in the current study. This did not appear to be the case as sex differences in twins and singletons were comparable (5.66% and 6.40% for singletons and twins, respectively). This difference is smaller than that reported in children (11%) (De Bellis et al. 2001) and adults (10–14.6%) (Gur et al. 1999; Nopoulos et al. 2000), suggesting that males experience accelerated brain growth in the first several years of life when compared with females. Accelerated brain growth in males in the postnatal period might be mediated by the neonatal testosterone surge. Males are born with elevated testosterone levels, as a result of the sudden drop in inhibitory estrogen produced by the placenta. Testosterone rapidly decreases in the first day of life and then begins to rise again after the first week, peaking around the third to fourth months of life and then dropping back to very low levels by 1 year of age (Forest et al. 1974; Fechner 2003). It is interesting to note that one of the most consistent anatomical findings in young children with autism, a condition with a marked male bias, is that they have larger-than-average brains, and that this difference emerges in the first year of life (Hazlett et al. 2005). It has been hypothesized that high levels of prenatal testosterone increase the risk for autism (Baron-Cohen et al. 2005, 2011; Knickmeyer and Baron-Cohen 2006), but no research has addressed the possible role of neonatal testosterone exposure as a risk factor.

TBM revealed localized sex differences in GM volume that are similar to those reported in adults in the right putamen (larger in males) and the anterior cingulate (larger in females). Sexual dimorphism in the putamen may be related to differences in basal ganglia function between males and females, particularly as regards striatal dopamine release (Munro et al. 2006), and may account for the higher prevalence of males in neuropsychiatric disorders related to basal ganglia dysfunction, such as ADHD (Qiu et al. 2009) and substance abuse (White 1996). Although we did not see an association with CAG repeat length or digit ratio and putamen volumes, amniotic testosterone predicts increased behavioral approach tendencies in peripubertal children by biasing reward-related regions, including the putamen, to be more responsive to positive rather than negatively valenced cues (Lombardo, Ashwin, Auyeung, Chakrabarti, Lai, et al. 2012). The anterior cingulate cortex (ACC) is involved in diverse cognitive and emotional processes including pain perception, reward-processing, conflict-monitoring, error-detection, and theory of mind. It has been suggested that the varied tasks that activate the ACC can be unified by the concept of self-regulation (Posner et al. 2007). Given this, it is interesting to note that newborn girls have a greater capacity for self-regulation than newborn boys (Weinberg et al. 1999; Lundqvist and Sabel 2000; Lundqvist 2001; Boatella-Costa et al. 2007).

Regarding pattern 2, our automated lobar morphometry analyses did not reveal relatively larger volumes of occipital GM or cerebellum in males, which were recently reported in a study of 325 children (ages 4.5–18 years) that also used automated lobar volumetry, suggesting that these sex differences arise postnatally, perhaps as a consequence of neonatal testosterone exposure. Regarding TBM analyses, localized sex differences that are present in children and adults, but absent in the neonate, are primarily in regions associated with social cognition [e.g. orbitofrontal cortex (Stone et al. 1998; Bachevalier and Loveland 2006) (female > male), right temporoparietal junction/posterior superior temporal sulcus (Saxe and Powell 2006; Decety and Lamm 2007; Nummenmaa and Calder 2009), and amygdala (Bachevalier and Loveland 2006; Adolphs 2010) (male > female)] and language [e.g. Heschl's gyrus (Wong et al. 2008) and planum temporale (Shapleske et al. 1999) (female > male)]. This was somewhat surprising given that newborn girls show better social interactive capacities than newborn boys on the Brazelton Scale (Lundqvist and Sabel 2000; Boatella-Costa et al. 2007) and also show a visual preference for a human face over a mechanical mobile, while newborn boys show the reverse (Connellan et al. 2001). There is also a small, but robust, female advantage in emotion expression recognition from infancy onwards (McClure 2000) and females lead males in early communicative gestures, productive vocabulary, word–gesture combinations, and word–word combinations (Ozcaliskan and Goldin-Meadow 2010; Eriksson et al. 2012). In addition, all of the sexually dimorphic regions above, with the exception of the amygdala, were associated with amniotic testosterone levels in a sample of peripubertal children (Lombardo, Ashwin, Auyeung, Chakrabarti, Taylor, et al. 2012). We hypothesize that fetal testosterone may bias the attention of newborn girls toward social stimuli, resulting in a richer learning environment for social cognition and language that promotes the development of these regions in a sexually dimorphic manner. Sex differences in the amygdala may arise through an independent process related to X-chromosome dosage, as females with Turner syndrome (X-monosomy) have enlarged amygdalae (Good et al. 2003) and males with Klinefelter syndrome (XXY) have smaller amygdalae (Patwardhan et al. 2002).

Regarding pattern 3, our findings of greater volumes of the bilateral medial temporal cortex (including parahippocampus and hippocampus) and anterior superior, middle, and inferior temporal gyri in males appear similar to previous reports in adults (Good et al. 2001; Chen et al. 2007), as do our findings of greater volumes in inferior frontal (Good et al. 2001) and primary motor cortices (Lentini et al. 2012) in females, although the literature is less consistent for the latter. In contrast, these dimorphisms were not present in a large peripubertal sample (Lombardo, Ashwin, Auyeung, Chakrabarti, Taylor, et al. 2012). Inconsistencies between studies may reflect differences in methodology or characteristics of the study populations, but we suggest that these findings may also indicate a relationship with circulating testosterone levels. As discussed previously, infant males experience a surge in testosterone levels. The gonads are then relatively quiescent until the onset of puberty when testosterone begins to climb again peaking in adolescence/early adulthood. GM volumes in the parahippocampus are positively correlated with testosterone in adults (Lentini et al. 2012). Regional GM was inversely correlated with testosterone in the left inferior frontal gyrus in a study of young adults (Witte et al. 2010), and greater androgen receptor efficiency in female adolescents is associated with a more masculine pattern of cortical maturation (i.e. increase of loss) in the left inferior frontal gyrus (Raznahan et al. 2010). Unfortunately, no direct measures of circulating testosterone at the time of MRI were available in our sample.

Regarding pattern 4, the majority of our findings appear to be unique to the neonatal period. This includes the findings of greater volumes in the fusiform gyri, left anterior supplementary motor area, rolandic opercula, insular cortex, and Heschl's gyri in males and greater volumes of the dorsolateral prefrontal cortex, visual cortex, posterior supplementary motor areas, and paracentral lobules in females. Whether these differences impact function in the short or long term remains to be elucidated. In the case of the dorsolateral prefrontal and visual cortices, it is interesting to note that sexual dimorphism in the opposite direction has been reported in peripubertal children. This could indicate accelerated maturation of these areas in females. A longitudinal study of brain development from age 4 to 20 has revealed that GM follows an inverted U-shaped trajectory with females peaking earlier than males in many regions (Giedd et al. 1999). This would manifest as a female greater than male difference in early development, when the dominant maturational processes are growth related (synapotogenesis, gliogenesis, dendritic branching, and axonal growth), but a male greater than female difference in late childhood/early adolescence, when the dominant maturational process is cortical thinning (perhaps as a consequence of dendritic pruning). There is functional evidence that the visual system matures earlier in females. Infant girls show earlier binocular function (Gwiazda et al. 1989), higher and earlier rates of habituation in response to smaller visual changes (Creighton 1984), and shorter latency EEG responses to visual pattern reversal (Malcolm et al. 2002).

These divergent spatiotemporal patterns suggest that multiple biological mechanisms contribute to sexual differentiation of the brain. We did explore one potential contributor, early androgen exposure. Androgen exposure and sensitivity, as indexed by the ratio of the second to fourth digit and by the number of CAG triplets in the androgen receptor gene, respectively, had some minor sex-specific effects on local GM volume, but did not appear to be the primary determinant of sexual dimorphism in this age group. However, we cannot rule out the possibility that a more direct measure of early testosterone exposure, such as amniotic testosterone, would have revealed significant effects. We also note that the utility of the digit ratio as a marker for individual differences in prenatal androgen exposure continues to be a matter of debate (Berenbaum et al. 2009; Breedlove 2010), and that a study of typically developing children such as this cannot directly test the possibility that sexual dimorphism in the neonate brain is determined by the presence or absence of testosterone in a binary manner.

In conclusion, we have demonstrated widespread sexual dimorphism in the neonate brain. As this is the first study of its kind, independent replication is critical. Comparison with the existing literature in children and adults suggests that sex is related to cortical development in a highly complex manner in terms of both spatial and temporal effects. It is likely that sexual dimorphism of the brain reflects the dynamic interplay of multiple mechanisms both biological (e.g. prenatal hormone production, neonatal hormone production, pubertal hormone production, direct sex-chromosome effects) and experiential (e.g. parental expectations and interactive behavior, exposure to physical hazards, culturally influenced lifestyle differences) (Rutter et al. 2003). Longitudinal designs which take account of all these factors are necessary to test detailed mechanistic hypotheses about the relationship between sex differences in brain development, cognitive function, and psychiatric risk.

Supplementary Material

Supplementary material can be found at: http://www.cercor.oxfordjournals.org/.

Funding

This work was supported by the National Institutes of Health (MH064065 and MH070890 to J.H.G., MH083045 to R.C.K., HD03110 and MH091645 to M.S., and RR025747, P01CA142538, MH086633, EB005149, and AG033387 to H.Z.) and by Autism Speaks.

Notes

We thank the participating families who made this project possible as well as the staff of the UNC MRI Research Center, the UNC NeuroImage Research and Analysis Laboratories, and the UNC Early Brain Development Program. *Conflict of Interest*: None declared.

References

Adolphs R. 2010. What does the amygdala contribute to social cognition? Ann N Y Acad Sci. 1191:42–61.

Allen RC, Zoghbi HY, Moseley AB, Rosenblatt HM, Belmont JW. 1992. Methylation of Hpaii and Hhai sites near the polymorphic CAG repeat in the human androgen-receptor gene correlates with X-chromosome inactivation. Am J Hum Genet. 51:1229–1239.

Bachevalier J, Loveland KA. 2006. The orbitofrontal-amygdala circuit and self-regulation of social-emotional behavior in autism. Neurosci Biobehav Rev. 30:97–117.

Baird G, Cox A, Charman T, Baron-Cohen S, Wheelwright S, Swettenham J, Drew A, Nightingale N. 2000. A screening instrument for autism at 18 months of age: a six year follow-up study. J Am Acad Child Adolesc Psychiatry. 39:694–702.

Baron-Cohen S, Knickmeyer RC, Belmonte MK. 2005. Sex differences in the brain: Implications for explaining autism. Science. 310:819–823.

Baron-Cohen S, Lombardo MV, Auyeung B, Ashwin E, Chakrabarti B, Knickmeyer R. 2011. Why are autism spectrum conditions more prevalent in males? Plos Biol. 9:e1001081.

BDCG (Brain Development Cooperative Group). 2012. Total and regional brain volumes in a population-based normative sample from 4 to 18 years: the NIH MRI Study of Normal Brain Development. Cereb Cortex. 22:1–12.

Bebbington P, Dunn G, Jenkins R, Lewis G, Brugha T, Farrell M, Heltzer M. 1998. The influence of age and sex on the prevalence of depressive conditions: report from the National Survey of Psychiatric Morbidity. Psychol Med. 28:9–19.

Berenbaum SA, Bryk KK, Nowak N, Quigley CA, Moffat S. 2009. Fingers as a marker of prenatal androgen exposure. Endocrinology. 150:5119–5124.

Boatella-Costa E, Costas-Moragas C, Botet-Mussons F, Fornieles-Deu A, De Caceres-Zurita ML. 2007. Behavioral gender differences in the neonatal period according to the Brazelton scale. Early Hum Dev. 83:91–97.

Breedlove SM. 2010. Minireview: organizational hypothesis: instances of the fingerpost. Endocrinology. 151:4116–4122.

Breedlove SM. 1994. Sexual differentiation of the human nervous system. Ann Rev Psychol. 45:389–418.

Brody BA, Kinney HC, Kloman AS, Gilles FH. 1987. Sequence of central nervous system myelination in human infancy. I. An autopsy study of myelination. J Neuropathol Exp Neurol. 46:283–301.

Cao J. 1999. The size of the connected components of excursion sets of chi(2), t and F fields. Adv Appl Probab. 31:579–595.
Caviness VS, Kennedy DN, Richelme C, Rademacher J, Filipek PA. 1996. The human brain age 7–11 years: a volumetric analysis based on magnetic resonance images. Cereb Cortex. 6:726–736.
Chakrabarti S, Fombonne E. 2001. Pervasive developmental disorders in preschool children. J Am Med Assoc. 285:3093–3099.
Chang C. 2002. Androgens and androgen receptor: mechanisms, functions, and clinical application. Boston: Kluwer Academic Publishers.
Chen XH, Sachdev PS, Wen W, Anstey KJ. 2007. Sex differences in regional gray matter in healthy individuals aged 44–48 years: a voxel-based morphometric study. Neuroimage. 36:691–699.
Connellan J, Baron-Cohen S, Wheelwright S, Ba'tki A, Ahluwalia J. 2001. Sex differences in human neonatal social perception. Infant Behav Develop. 23:113–118.
Cox RW. 1996. AFNI: software for analysis and visualization of functional magnetic resonance neuroimages. Comput Biomed Res. 29:162–173.
Creighton DE. 1984. Sex differences in the visual habituation of 4-, 6-, and 8-month-old infants. Infant Behav Develop. 7:237–249.
De Bellis MD, Keshavan MS, Beers SR, Hall J, Frustaci K, Masalehdan A, Noll J, Boring AM. 2001. Sex differences in brain maturation during childhood and adolescence. Cereb Cortex. 11:552–557.
Decety J, Lamm C. 2007. The role of the right temporoparietal junction in social interaction: how low-level computational processes contribute to meta-cognition. Neuroscientist. 13:580–593.
Dekaban AS, Sadowsky D. 1978. Changes in brain weights during the span of human life: relation of brain weights to body heights and body weights. Ann Neurol. 4:345–356.
Eriksson M, Marschik PB, Tulviste T, Almgren M, Perez Pereira M, Wehberg S, Marjanovic-Umek L, Gayraud F, Kovacevic M, Gallego C. 2012. Differences between girls and boys in emerging language skills: evidence from 10 language communities. Br J Dev Psychol. 30:326–343.
Fatemi SH, Folsom TD. 2009. The neurodevelopmental hypothesis of schizophrenia, revisited. Schizophr Bull. 35:528–548.
Fechner PY. 2003. The biology of puberty: new developments in sex differences. In: Hayward C, editor. Gender differences at puberty. Cambridge: Cambridge University Press. p. 17–28.
Filipek PA. 1999. Neuroimaging in the developmental disorders: the state of the science. J Child Psychol Psyc. 40:113–128.
Filipek PA, Richelme C, Kennedy DN, Caviness VS. 1994. Young-adult human brain—an MRI-based morphometric analysis. Cereb Cortex. 4:344–360.
Forest MG, Sizonenko PC, Cathiard AM, Bertrand J. 1974. Hypophyso-gonadal function in humans during the first year of life: I. Evidence for testicular activity in early infancy. J Clin Invest. 53:819–828.
Giedd JN, Blumenthal J, Jeffries NO, Castellanos FX, Liu H, Zijdenbos A, Paus T, Evans AC, Rapoport JL. 1999. Brain development during childhood and adolescence: a longitudinal MRI study. Nat Neurosci. 2:861–863.
Giedd JN, Castellanos FX, Rajapakse JC, Vaituzis AC, Rapoport JL. 1997. Sexual dimorphism of the developing human brain. Prog Neuropsychopharmacol Biol Psychiatry. 21:1185–1201.
Giedd JN, Snell JW, Lange N, Rajapakse JC, Casey BJ, Kozuch PL, Vaituzis AC, Vauss YC, Hamburger SD, Kaysen D et al. 1996. Quantitative magnetic resonance imaging of human brain development: ages 4–18. Cereb Cortex. 6:551–560.
Gilmore JH, Kang C, Evans DD, Wolfe HM, Smith JK, Lieberman JA, Lin W, Hamer RM, Styner M, Gerig G. 2010. Prenatal and neonatal brain structure and white matter maturation in children at high risk for schizophrenia. Am J Psychiatry. 167:1083–1091.
Gilmore JH, Lin W, Prastawa MW, Looney CB, Vetsa YSK, Knickmeyer RC, Evans DD, Smith JK, Hamer RM, Lieberman JA et al. 2007. Regional gray matter growth, sexual dimorphism, and cerebral asymmetry in the neonatal brain. J Neurosci. 27:1255–1260.
Gilmore JH, Shi F, Woolson SL, Knickmeyer RC, Short SJ, Lin W, Zhu H, Hamer RM, Styner M, Shen D. 2012. Longitudinal development of cortical and subcortical gray matter from birth to 2 years. Cereb Cortex. 22:2478–2485.
Goldstein JM, Seidman LJ, Horton NJ, Makris N, Kennedy DN, Caviness Jnr VS, Faraone SV, Tsuang MT. 2001. Normal sexual dimorphism of the adult human brain assessed by in vivo magnetic resonance imaging. Cereb Cortex. 11:490–497.
Good CD, Johnsrude I, Ashburner J, Henson RNA, Friston KJ, Frackowiak RSJ. 2001. Cerebral asymmetry and the effects of sex and handedness on brain structure: a voxel-based morphometric analysis of 465 normal adult human brains. Neuroimage. 14:685–700.
Good CD, Lawrence K, Thomas NS, Price CJ, Ashburner J, Friston KJ, Frackowiak RSJ, Oreland L, Skuse DH. 2003. Dosage-sensitive X-linked locus influences the development of amygdala and orbitofrontal cortex, and fear recognition in humans. Brain. 126:2431–2446.
Gur RC, Turetsky BI, Matsui M, Yan M, Bilker W, Hughett P, Gur RE. 1999. Sex differences in brain gray and white matter in healthy young adults: correlations with cognitive performance. J Neurosci. 19:4065–4072.
Gwiazda J, Bauer J, Held R. 1989. Binocular function in human infants: correlation of stereoptic and fusion-rivalry discriminations. J Pediatr Ophthalmol Strabismus. 26:128–132.
Hayasaka S, Phan KL, Liberzon I, Worsley KJ, Nichols TE. 2004. Nonstationary cluster-size inference with random field and permutation methods. Neuroimage. 22:676–687.
Hazlett HC, Poe M, Gerig G, Smith RG, Provenzale J, Ross A, Gilmore J, Piven J. 2005. Magnetic resonance Imaging and head circumference study of brain size in autism—birth through age 2 years. Arch Gen Psychiatry. 62:1366–1376.
Hazlett HC, Poe MD, Gerig G, Styner M, Chappell C, Smith RG, Vachet C, Piven J. 2011. Early brain overgrowth in autism associated with an increase in cortical surface area before age 2 years. Arch Gen Psychiatry. 68:467–476.
Hua X, Leow AD, Parikshak N, Lee S, Chiang MC, Toga AW, Jack CR Jr, Weiner MW, Thompson PM. 2008. Tensor-based morphometry as a neuroimaging biomarker for Alzheimer's disease: an MRI study of 676 AD, MCI, and normal subjects. Neuroimage. 43:458–469.
Huttenlocher PR, Dabholkar AS. 1997. Regional differences in synaptogenesis in human cerebral cortex. J Comp Neurol. 387:167–178.
Joshi S, Davis B, Jomier M, Gerig G. 2004. Unbiased diffeomorphic atlas construction for computational anatomy. Neuroimage. 23 (Suppl 1):S151–S160.
Kagan J, Herschkowitz N. 2005. A young mind in a growing brain. Mahwah (NJ): Erlbaum Associates.
Kasprian G, Brugger PC, Weber M, Krssak M, Krampl E, Herold C, Prayer D. 2008. In utero tractography of fetal white matter development. Neuroimage. 43:213–224.
Knickmeyer RC, Baron-Cohen S. 2006. Fetal testosterone and sex differences in typical social development and in autism. J Child Neurol. 21:825–845.
Knickmeyer RC, Gouttard S, Kang C, Evans D, Wilber K, Smith JK, Hamer RM, Lin W, Gerig G, Gilmore JH. 2008. A structural MRI study of human brain development from birth to 2 years. J Neurosci. 28:12176–12182.
Knickmeyer RC, Woolson S, Hamer RM, Konneker T, Gilmore JH. 2011. 2D:4D ratios in the first 2 years of life: stability and relation to testosterone exposure and sensitivity. Horm Behav. 60:256–263.
Lentini E, Kasahara M, Arver S, Savic I. 2012. Sex differences in the human brain and the impact of sex chromosomes and sex hormones. Cereb Cortex. [epub ahead of print].
Lepore N, Brun C, Chou YY, Chiang MC, Dutton RA, Hayashi KM, Luders E, Lopez OL, Aizenstein HJ, Toga AW et al. 2008. Generalized tensor-based morphometry of HIV/AIDS using multivariate statistics on deformation tensors. IEEE Trans Med Imaging. 27:129–141.
Li Y, Gilmore JH, Shen D, Styner M, Lin W, Zhu H. 2013. Multiscale adaptive generalized estimating equations for longitudinal neuroimaging data. Neuroimage. 72:91–105.
Li YM, Zhu HT, Shen DG, Lin WL, Gilmore JH, Ibrahim JG. 2011. Multiscale adaptive regression models for neuroimaging data. J Roy Stat Soc B. 73:559–578.

Liang KY, Zeger SL. 1986. Longitudinal Data-Analysis Using Generalized Linear-Models. Biometrika. 73:13–22.
Lombardo MV, Ashwin E, Auyeung B, Chakrabarti B, Lai MC, Taylor K, Hackett G, Bullmore ET, Baron-Cohen S. 2012. Fetal programming effects of testosterone on the reward system and behavioral approach tendencies in humans. Biol Psychiatry. 72:839–847.
Lombardo MV, Ashwin E, Auyeung B, Chakrabarti B, Taylor K, Hackett G, Bullmore ET, Baron-Cohen S. 2012. Fetal testosterone influences sexually dimorphic gray matter in the human brain. J Neurosci. 32:674–680.
Lucas A, Beard C, O'Fallon W, Kurland L. 1991. Fifty-year trends in the incidence of anorexia nervosa in Rochester, Minnesota: a population-based study. Am J Psychiatry. 148:917–922.
Lundqvist C. 2001. Correlation between level of self-regulation in the newborn infant and developmental status at two years of age. Acta Paediatr. 90:345–350.
Lundqvist C, Sabel KG. 2000. Brief report: The Brazelton Neonatal Behavioral Assessment Scale detects differences among newborn infants of optimal health. J Pediatr Psychol. 25:577–582.
Malcolm CA, McCulloch DL, Shepherd AJ. 2002. Pattern-reversal visual evoked potentials in infants: gender differences during early visual maturation. Dev Med Child Neurol. 44:345–351.
Manning JT, D. S, Wilson JD, Lewis-Jones DI. 1998. The ratio of 2nd to 4th digit length: a predictor of sperm numbers and levels of testosterone, LH and Oestrogen. Hum Reprod. 13:3000–3004.
McCarthy MM, Arnold AP. 2011. Reframing sexual differentiation of the brain. Nat Neurosci. 14:677–683.
McClure EB. 2000. A meta-analytic review of sex differences in facial expression processing and their development in infants, children, and adolescents. Psychol Bull. 126:424–453.
McLean C, Asnaani A, Litz B, Hofmann S. 2011. Gender differences in anxiety disorders: prevalence, course of illness, comorbidity and burden of illness. J Psychiatr Res. 45:1027–1035.
Moffitt TE. 1990. Juvenile-delinquency and attention deficit disorder—boys developmental trajectories from age 3 to age 15. Child Dev. 61:893–910.
Moffitt TE, Caspi A. 2001. Childhood predictors differentiate life-course persistent and adolescence-limited antisocial pathways among males and females. Dev Psychopathol. 13:355–375.
Munoz A, Rosner B, Carey V. 1986. Regression-analysis in the presence of heterogeneous intraclass correlations. Biometrics. 42:653–658.
Munro CA, McCaul ME, Wong DF, Oswald LM, Zhou Y, Brasic J, Kuwabara H, Kumar A, Alexander M, Ye W et al. 2006. Sex differences in striatal dopamine release in healthy adults. Biol Psychiatry. 59:966–974.
Nopoulos P, Flaum M, Andreasen NC. 1997. Sex differences in brain morphology in schizophrenia. Am J Psychiatry. 154:1648–1654.
Nopoulos P, Flaum M, O'Leary D, Andreasen NC. 2000. Sexual dimorphism in the human brain: evaluation of tissue volume, tissue composition and surface anatomy using magnetic resonance imaging. Psychiatry Res. 98:1–13.
Nummenmaa L, Calder AJ. 2009. Neural mechanisms of social attention. Trends Cogn Sci. 13:135–143.
Ozcaliskan S, Goldin-Meadow S. 2010. Sex differences in language first appear in gesture. Dev Sci. 13:752–760.
Patwardhan AJ, Brown WE, Bender BG, Linden MG, Eliz S, Reiss AL. 2002. Reduced size of the amygdala in individuals with 47,XXY and 47,XXX Karyotypes. Am J Med Genet. 114:93–98.
Petanjek Z, Judas M, Kostovic I, Uylings HBM. 2008. Lifespan alterations of basal dendritic trees of pyramidal neurons in the human prefrontal cortex: a layer-specific pattern. Cereb Cortex. 18:915–929.
Posner MI, Rothbart MK, Sheese BE, Tang Y. 2007. The anterior cingulate gyrus and the mechanism of self-regulation. Cogn Affect Behav Neurosci. 7:391–395.
Prastawa M, Gilmore JH, Lin WL, Gerig G. 2005. Automatic segmentation of MR images of the developing newborn brain. Med Image Anal. 9:457–466.
Qiu A, Crocetti D, Adler M, Mahone EM, Denckla MB, Miller MI, Mostofsky SH. 2009. Basal ganglia volume and shape in children with attention deficit hyperactivity disorder. Am J Psychiatry. 166:74–82.
Rapoport JC, Addington AM, Frangou S. 2005. The neurodevelopmental model of schizophrenia: update 2005. Mol Psychiatry. 10:439–449.
Raznahan A, Lee Y, Stidd R, Long R, Greenstein D, Clasen L, Addington A, Gogtay N, Rapoport JL, Giedd JN. 2010. Longitudinally mapping the influence of sex and androgen signaling on the dynamics of human cortical maturation in adolescence. Proc Natl Acad Sci USA. 107:16988–16993.
Reiss AL, Abrams MT, Singer HS, Ross JL, Denckla MB. 1996. Brain development, gender and IQ in children—a volumetric imaging study. Brain. 119:1763–1774.
Remschmidt H, Schulz E, Martin M, Warnke A, Trott G. 1994. Childhood-onset schizophrenia: history of the concept and recent studies. Schizophr Bull. 20:727–745.
Rijpkema M, Everaerd D, van der Pol C, Franke B, Tendolkar I, Fernandez G. 2012. Normal sexual dimorphism in the human basal ganglia. Hum Brain Mapp. 33:1246–1252.
Rutter M, Caspi A, Moffitt TE. 2003. Using sex differences in psychopathology to study causal mechanisms: unifying issues and research strategies. J Child Psychol Psychiatry. 44:1092–1115.
Saxe R, Powell LJ. 2006. It's the thought that counts: specific brain regions for one component of theory of mind. Psychol Sci. 17:692–699.
Shapleske J, Rossell SL, Woodruff PW, David AS. 1999. The planum temporale: a systematic, quantitative review of its structural, functional and clinical significance. Brain Res Brain Res Rev. 29:26–49.
Stone VE, Baron-Cohen S, Knight RT. 1998. Frontal lobe contributions to theory of mind. J Cogn Neurosci. 10:640–656.
Szatmari P, Offord DR, Boyle MH. 1989. Ontario child health study—prevalence of attention deficit disorder with hyperactivity. J Child Psychol Psychiatry. 30:219–230.
Wang HS, Kuo MF. 2003. Tourette's syndrome in Taiwan: an epidemiological study of tic disorders in an elementary school at Taipei County. Brain Dev. 25:S29–S31.
Weinberg MK, Tronick EZ, Cohn JF, Olson KL. 1999. Gender differences in emotional expressivity and self-regulation during early infancy. Dev Psychol. 35:175–188.
White NM. 1996. Addictive drugs as reinforcers: multiple partial actions on memory systems. Addiction. 91:921–949; discussion 951–965.
Witte AV, Savli M, Holik A, Kasper S, Lanzenberger R. 2010. Regional sex differences in grey matter volume are associated with sex hormones in the young adult human brain. Neuroimage. 49:1205–1212.
Wolff JJ, Gu H, Gerig G, Elison JT, Styner M, Gouttard S, Botteron KN, Dager SR, Dawson G, Estes AM et al. 2012. Differences in white matter fiber tract development present from 6 to 24 months in infants with autism. Am J Psychiatry. 169:589–600.
Wong PC, Warrier CM, Penhune VB, Roy AK, Sadehh A, Parrish TB, Zatorre RJ. 2008. Volume of left Heschl's Gyrus and linguistic pitch learning. Cereb Cortex. 18:828–836.
Worsley KJ, Andermann M, Koulis T, MacDonald D, Evans AC. 1999. Detecting changes in nonisotropic images. Hum Brain Mapp. 8:98–101.
Worsley KJ, Marrett S, Neelin P, Vandal AC, Friston K, Evans AC. 1996. A unified statistical approach for determining significant voxels in images of cerebral activation. Hum Brain Mapp. 4:58–73.
Yushkevich PA, Piven J, Hazlett HC, Smith RG, Ho S, Gee JC, Gerig G. 2006. User-guided 3D active contour segmentation of anatomical structures: significantly improved efficiency and reliability. Neuroimage. 31:1116–1128.
Zhu HT, Li Y, Ibrahim JG, Lin W, Shen DG. 2009. MARM: multiscale adaptive regression for neuroimaging data. Inf Process Med Imaging. 21:314–325.